Constraint on Lorentz Invariance Violation for spectral lag transition in GRB 160625B using profile likelihood

Shantanu Desai[1*] and Shalini Ganguly[2†]

[1]*Department of Physics, IIT Hyderabad, Kandi, Telangana-502284, India and*
[2]*Department of Physics, St. Mary's College of Maryland, St. Mary's City, MD, 20686, USA*

We reanalyze the spectral lag data for of GRB 160625B using frequentist inference to constrain the energy scale (E_{QG}) of Lorentz Invariance Violation (LIV). For this purpose, we use profile likelihood to deal with the astrophysical nuisance parameters. This is in contrast to Bayesian inference implemented in previous works, where marginalization was carried out over the nuisance parameters. We show that with profile likelihood, we do not find a global minimum for χ^2 as a function of E_{QG} below the Planck scale for both the linear and quadratic models of LIV, whereas bounded credible intervals were obtained using Bayesian inference. Therefore, we can set lower limits in a straightforward manner. We find that $E_{QG} \geq 3.7 \times 10^{16}$ GeV and $E_{QG} \geq 2.6 \times 10^{7}$ GeV at 68% c.l., for linear and quadratic LIV, respectively. Therefore, this is the first proof of principles application of profile likelihood method to the analysis of GRB spectral lag data to constrain LIV.

I. INTRODUCTION

The spectral lags of Gamma-ray Bursts (GRBs) have been widely used [1–3] as a probe of Lorentz invariance Violation (LIV) ever since this was first proposed more than two decades ago [4]. The spectral lag is defined as the time difference between the arrival of high energy and low energy photons, and is positive if the high energy photons precede the low energy ones. In case of LIV caused by an energy-dependent speed of light, one expects a turnover in the spectral lag data at high energies.

Among the plethora of searches for LIV using GRBs, the first work which found a turnover in the spectral lag data was by Wei et al. [5] (W17, hereafter). This analysis found evidence for a transition from positive to negative time lag in the spectral lag data for GRB 160625B, by using the data from Fermi-LAT and Fermi-GBM. By modeling the time lag as sum of intrinsic astrophysical time-lag and an energy-dependent speed of light, which kicks in at high energies, they argued that this observation constitutes a robust evidence for a turnover in the spectral lag data. Statistical significance of this turnover was then calculated using frequentist, information theory and Bayesian model selection techniques [6, 7]. Using Bayesian inference, lower limits on the quantum gravity energy scale was set at 0.5×10^{16} GeV and 1.4×10^{7} GeV for linear and quadratic LIV, respectively [5]. These limits were obtained by marginalizing over the astrophysical nuisance parameters. All other analyses searching for LIV using GRB spectral lags have always used Bayesian inference. These include some of our own past works [8–10].

In this work we redo the analysis in [5] using frequentist inference, where we deal with the nuisance astro-

physical parameters using profile likelihood. While the profile likelihood is a "bread and butter" tool in experimental high energy Physics [11], until recently it has seldom been used in Astrophysics, where Bayesian inference is commonly used. Recently, however there has been a renaissance in the use of Profile likelihood in the field of Cosmology (see [12–16] for an incomplete list). In particular it was shown that one reach opposite conclusions for the fraction of Early Dark energy using Profile Likelihood as compared to Bayesian inference [12].

The outline of this manuscript is as follows. We review the basic data analysis done in W17 to search for LIV in Section II. We compare the contrast Bayesian and frequentist parameter estimation highlighting how these methods handle nuisance parameters in Sect. III. Our results and conclusions can be found in Sect. IV and Sect. V respectively.

II. DATA AND MODEL FOR SPECTRAL TIME LAGS

The observed spectral time lag from a given GRB can be written down as :

$$\Delta t_{obs} = \Delta t_{int} + \Delta t_{LIV}, \quad (1)$$

where Δt_{int} is the intrinsic time lag between the emission of photon of a particular energy and the lowest energy photon from the GRB and Δt_{LIV} is the LIV-induced time-lag. W17 used the following model for the intrinsic emission delay:

$$\Delta t_{int}(E)(\sec) = \tau \left[\left(\frac{E}{keV} \right)^{\alpha} - \left(\frac{E_0}{keV} \right)^{\alpha} \right], \quad (2)$$

where E_0=11.34 keV; whereas τ and α are free parameters. This model has been subsequently used in other searches for LIV [1]. The remaining LIV-induced time lag in Eq. 1 (Δt_{LIV}) can be written for sub-luminal LIV

as [17]:

$$\Delta t_{LIV} = -\frac{1+n}{2H_0}\frac{E^n - E_0^n}{E_{QG,n}^n}\int_0^z \frac{(1+z')^n dz'}{\sqrt{\Omega_M(1+z')^3 + 1 - \Omega_M}},$$
(3)

where $E_{QG,n}$ is the Lorentz-violating or quantum gravity scale, above which Lorentz violation kicks in; H_0 is the Hubble constant and Ω_M is the cosmological matter density. W17 considered two different models for LIV, which have $n = 1$ and $n = 2$, corresponding to linear and quadratic LIV, respectively. For the cosmological parameters in Eq. 3, W17 used $H_0 = 67.3$ km/sec/Mpc and $\Omega_m = 0.315$.

W17 considered the spectra lags for GRB 160625B, located at redshift of $z = 1.41$. W17 collated 37 spectral lags using data from Fermi-GBM and Fermi-LAT relative to the lowest energy band of 10-12 keV, extending up to 20 MeV (cf. Table 1 of W17). W17 then used Bayesian inference, where the sampling of the posterior was done using Markov Chain Monte Carlo (MCMC). W17 obtained lower limit on E_{QG} given by $E_{QG} \geq 0.5 \times 10^{16}$ GeV and $E_{QG} \geq 1.4 \times 10^7$ GeV for linear and quadratic LIV, respectively, at 1σ. A similar Bayesian parameter estimation for the same dataset using Variational Inference was done in [7]. Using both these methods, one obtained closed 1σ intervals for E_{QG}, implying that prima-facie a central interval should be quoted for E_{QG} instead of a one-sided lower limit.

III. COMPARISON OF BAYESIAN AND FREQUENTIST INFERENCE

We provide a very brief primer on Bayesian and frequentist parameter estimation and highlight some of the differences between the two methods for our particular use case. More details on Bayesian parameter estimation can be found in recent reviews [18–20]. Frequentist parameter estimation is usually reviewed in PDG, with the latest update in [11].

For both these methods, one needs to model the probability of the data (D) given a parametric function consisting of parameter vector (θ). We denote this probability by $P(D|\theta)$. For our example, this has been modeled by a Gaussian likelihood ($\mathcal{L}(\theta)$) as follows:

$$P(D|\theta) = \mathcal{L}(\theta) = \prod_{i=1}^{N} \frac{1}{\sigma_i\sqrt{2\pi}}\exp\left\{-\frac{[\Delta t_i - f(\Delta E_i, \theta)]^2}{2\sigma_i^2}\right\},$$
(4)

where N is the total number of data points; Δt_i denotes the data which correspond to the observed spectral lags, and σ_i denotes the observed uncertainty in the spectral lag. The function $f(\Delta E_i, \theta)$ is obtained from the sum of Eq. 2 and Eq. 3.

In Bayesian inference, one evaluates the Bayesian Posterior $P(\theta|D)$ which is given by $P(\theta|D) \propto P(D|\theta)P(\theta)$, where $P(\theta)$ is the prior on parameter vector θ. Bayesian

parameter inference then entails obtaining central estimates from the posterior probability distribution. In practice, almost all Bayesian computations are nowadays done using MCMC (although see [7]), and the median estimator along with the 68 percentile intervals are computed to obtain 1σ intervals [19].

Usually the parameter vector θ consists of more than one free parameter. Among these, we might be most interested in only one of the parameters. In such cases, the other free parameters can be considered as nuisance parameters. For our use case, θ consists of three parameters: $\{E_{QG}, \tau, \alpha\}$. Since we are mainly interested in constraining E_{QG}, the astrophysical parameters τ and α can be considered as nuisance parameters. For the sake of illustration, let us assume that in a geric setting the parameter vector (θ) consists of two parameters: $\theta = \{\phi, \alpha\}$. Among these, let us consider ϕ to be the parameter of interest and α to be the nuisance parameter. In Bayesian inference, the central estimates for ϕ are obtained by integrating the posterior over the nuisance parameter α to get the posterior distribution for $P(\phi)$.

$$P(\phi) = \int P(\phi, \alpha|D)d\alpha,$$
(5)

where $P(\phi, \alpha|D)$ is the posterior for θ. The central estimates and error intervals are obtained from $P(\phi)$. All works on searches for LIV and setting constraints on E_{QG} have always followed the above prescription [1].

To deal with nuisance parameters in frequentist statistics on the other hand, one calculates the profile likelihood, obtained by maximizing the combined likelihood $\mathcal{L}(\phi, \alpha)$ with respect to α:

$$\mathcal{L}(\phi) = \max_{\alpha}\mathcal{L}(\phi, \alpha)$$
(6)

The central estimate for ϕ can then be obtained from $\mathcal{L}(\phi)$. In practice, one defines $\chi^2(\phi) = -2\ln\mathcal{L}(\phi)$ and the frequentist confidence intervals are constructed from $\Delta\chi^2(\phi) = \chi^2(\phi) - \chi^2_{min}$, where χ^2_{min} is the global minimum for $\chi^2(\phi)$. If χ^2_{min} is far from the physical boundary, the central interval for the parameter ϕ at a given confidence level can be obtained using Newman prescription from the $\Delta\chi^2$ intercept [21]. Close to the physical boundary one must use the Feldman-Cousins prescription [22].

This method of profile likelihood has many potential differences compared to the Bayesian counterpart [23]. The profile likelihood does not require priors unlike Bayesian inference, which could affect the final results. The profile likelihood formalism also allows us to include the effect of physical boundary using the Feldman-Cousins prescription [22]. The profile likelihood also does not suffer from the volume effect, which could arise in marginalization [24]. Other advantages of profile likelihood over Bayesian analyses have been extensively discussed in recent works related to parameter estimation in Cosmology [13, 16, 24]. Most recently, this concept of profiling over nuisance parameters has also been applied to the Bayesian posterior to define a "profile pos-

terior" [25, 26]. This is a hybrid method combining the tenets of both frequentist and Bayesian analysis.

We now apply the profile likelihood method to the spectral lag data for GRB 1606025B in order to constrain E_{QG}.

IV. APPLICATION OF PROFILE LIKELIHOOD TO GRB 1606025B SPECTRAL LAG DATA

For both linear and quadratic LIV, our parameter vector consists of three parameters $\{E_{QG}, \tau, \alpha\}$, where we are mostly interested in the estimates of E_{QG}. Therefore, τ and α can be considered as nuisance parameters. We use the same likelihood as in Eq. 4. To simplify the calculation of the profile likelihood using Eq. 6, we minimize χ^2 given by $\chi^2 \equiv -2\ln\theta$. We then construct a logarithmically spaced grid for E_{QG} from 10^6 to 10^{19} GeV. The upper bound of 10^{19} GeV corresponds to Planck scale and can be considered as the physical boundary. For each value of E_{QG} at this grid, we calculate the minimum $\chi^2(E_{QG})$ by minimizing over α and τ. For this purpose we used `scipy.optimize.fmin` function, which uses the Nelder-Mead simplex algorithm [21]. As a cross-check we also compared with the Powell minimization algorithm built in `scipy`, which gives the same results. We then plot $\Delta\chi^2$ as a function of E_{QG}, where $\Delta\chi^2 = \chi^2(E_{QG}) - \chi^2_{min}$. The corresponding $\Delta\chi^2$ curves as a function of E_{QG} can be found in Fig. 1 and Fig. 2 for linear and quadratic LIV, respectively. For both the LIV models we find that $\Delta\chi^2$ always decreasing with increasing E_{QG}. Here, χ^2_{min} corresponds to χ^2 at the Planck scale, which can be considered as the physical boundary. Therefore, there is no global minimum followed by a rising trend. This is different from previus results obtained using Bayesian inference, where closed 1σ intervals for E_{QG} were obtained after marginalizing over τ and α [5, 7].

Therefore, we can obtain a one-sided lower limit on E_{QG} in a seamless way. Based on the Newman prescription the 68.27% (68%, to shorten the notation) lower limit is given by value of E_{QG} for which $\Delta\chi^2 = 1$ [12, 21]. Therefore, the 68% lower limits $E_{QG} \geq 3.7 \times 10^{16}$ GeV and $E_{QG} \geq 2.6 \times 10^7$ GeV for linear and quadratic LIV, respectively. We note the E_{QG} values for $\Delta\chi^2 = 1$ are obtained far from the physical boundary, the Newman prescription suffices and there is no need to switch to the Feldman-Cousins prescription. Our lower limits for E_{QG} are comparable, although slightly higher than the Bayesian lower limits obtained in W17, corresponding 0.5×10^{16} GeV and 1.4×10^{16} GeV, for linear and quadratic LIV, respectively.

V. CONCLUSIONS

In this work we have reanalyzed the data for spectral lag transition in GRB 1606025B, using the frequen-
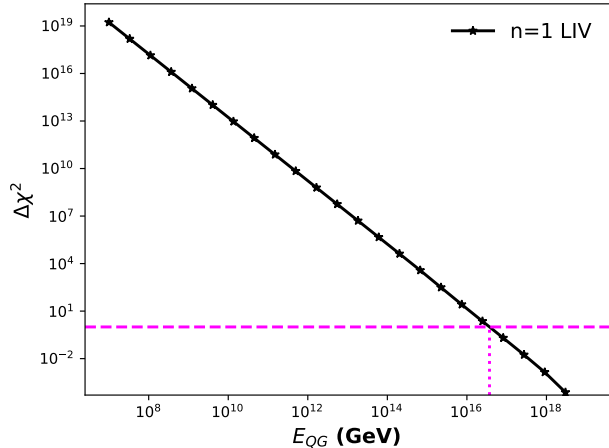
FIG. 1: $\Delta\chi^2$ (defined as $\chi^2 - \chi^2_{min}$) as a function of E_{QG} for linear LIV, corresponding to $n = 1$ in Eq. 3. The horizontal magenta dashed line is at $\Delta\chi^2 = 1$ and the corresponding X-intercept of the curves (magenta dotted line) gives the 68% c.l. lower limit at $E_{QG} = 3.7 \times 10^{16}$ GeV.
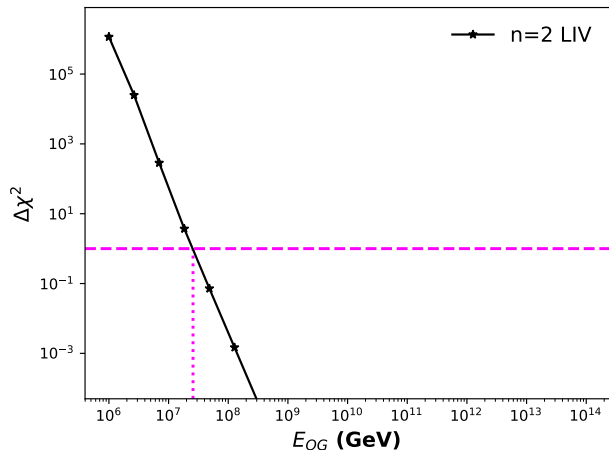
FIG. 2: $\Delta\chi^2$ (defined as $\chi^2 - \chi^2_{min}$) as a function of E_{QG} for quadratic LIV, corresponding to $n = 2$ in Eq. 3. The horizontal magenta dashed line is at $\Delta\chi^2 = 1$ and the corresponding X-intercept of the curves (magenta dotted line) gives the 68% c.l. lower limit at $E_{QG} = 2.6 \times 10^7$ GeV.

tist method of profile likelihood in order to constrain the energy scale for LIV. All previous searches for LIV using GRB spectral lags have used Bayesian inference, which involved marginalizing over the astrophysical nuisance parameters [5, 7]. Similar to previous works, we model the spectral lags as a sum of astrophysical induced time lag and LIV induced time lag. We consider the same parametric models for both the lags as in previous works [5–7]. The astrophysical induced lag (cf. Eq. 2) consists of two nuisance parameters, whereas the physically interesting parameter we want to constrain is the energy scale of LIV (denoted by E_{QG} in Eq. 3).

For both the LIV models, we calculated the $\Delta\chi^2$ as a function of E_{QG} by computing the minimum value of χ^2 over the astrophysical parameters for each value of E_{QG}. These plots of $\Delta\chi^2$ can be found in Fig 1 and 2 for linear and quadratic LIV, respectively. One difference compared to Bayesian inference inference is that we do not get a convex shape for the probability distribution for E_{QG} below the Planck scale using the profile likelihood method. Therefore, there is no global minimum and one can unhesitatingly set one-sided lower limits on E_{QG} for a given confidence level. The corresponding 68% lower limits on E_{QG} which we obtain are given by $E_{QG} \geq 3.7 \times 10^{16}$ GeV and $E_{QG} \geq 2.6 \times 10^7$ GeV for linear and quadratic LIV, respectively. These are slightly upper than the Bayesian lower limits obtained in W17.

Therefore, this the first proof of principles application of profile likelihood in the analysis of GRB spectral lag data to search for LIV and provides a seamless way to set a lower limit. In future works we shall apply this method to other searches for LIV using GRB spectral lags.

Acknowledgments

[1] S. Desai, in *Recent Progress on Gravity Tests. Challenges and Future Perspectives*, edited by C. Bambi and A. Cárdenas-Avendaño (2024), pp. 433–463.

[2] Y.-W. Yu, H. Gao, F.-Y. Wang, and B.-B. Zhang, in *Handbook of X-ray and Gamma-ray Astrophysics. Edited by Cosimo Bambi and Andrea Santangelo* (2022), p. 31.

[3] J.-J. Wei and X.-F. Wu, in *Handbook of X-ray and Gamma-ray Astrophysics. Edited by Cosimo Bambi and Andrea Santangelo* (2022), p. 82.

[4] G. Amelino-Camelia, J. Ellis, N. E. Mavromatos, D. V. Nanopoulos, and S. Sarkar, Nature (London) **393**, 763 (1998), astro-ph/9712103.

[5] J.-J. Wei, B.-B. Zhang, L. Shao, X.-F. Wu, and P. Mészáros, Astrophys. J. Lett. **834**, L13 (2017), 1612.09425.

[6] S. Ganguly and S. Desai, Astroparticle Physics **94**, 17 (2017), 1706.01202.

[7] G. Gunapati, A. Jain, P. K. Srijith, and S. Desai, PASA **39**, e001 (2022), 1803.06473.

[8] R. Agrawal, H. Singirikonda, and S. Desai, JCAP **2021**, 029 (2021), 2102.11248.

[9] S. Desai, R. Agrawal, and H. Singirikonda, European Physical Journal C **83**, 63 (2023), 2205.12780.

[10] V. Pasumarti and S. Desai, Journal of High Energy Astrophysics **40**, 41 (2023), 2307.02296.

[11] Particle Data Group, P. A. Zyla, R. M. Barnett, J. Beringer, O. Dahl, D. A. Dwyer, D. E. Groom, C. J. Lin, K. S. Lugovsky, E. Pianori, et al., Progress of Theoretical and Experimental Physics **2020**, 083C01 (2020).

[12] L. Herold, E. G. M. Ferreira, and E. Komatsu, Astrophys. J. Lett. **929**, L16 (2022), 2112.12140.

[13] P. Campeti and E. Komatsu, Astrophys. J. **941**, 110 (2022), 2205.05617.

[14] E. Ó. Colgáin, S. Pourojaghi, and M. M. Sheikh-Jabbari, arXiv e-prints arXiv:2406.06389 (2024), 2406.06389.

[15] T. Karwal, Y. Patel, A. Bartlett, V. Poulin, T. L. Smith, and D. N. Pfeffer, arXiv e-prints arXiv:2401.14225 (2024), 2401.14225.

[16] L. Herold, E. G. M. Ferreira, and L. Heinrich, arXiv e-prints arXiv:2408.07700 (2024), 2408.07700.

[17] U. Jacob and T. Piran, JCAP **1**, 031 (2008), 0712.2170.

[18] R. Trotta, ArXiv e-prints (2017), 1701.01467.

[19] S. Sharma, Annual Review of Astron. and Astrophys. **55**, 213 (2017), 1706.01629.

[20] A. Krishak and S. Desai, JCAP **2020**, 006 (2020), 2003.10127.

[21] W. H. Press, S. A. Teukolsky, W. T. Vetterling, and B. P. Flannery, *Numerical recipes in FORTRAN. The art of scientific computing* (1992).

[22] G. J. Feldman and R. D. Cousins, Phys. Rev. D **57**, 3873 (1998), physics/9711021.

[23] R. D. Cousins, American Journal of Physics **63**, 398 (1995).

[24] A. Gómez-Valent, Phys. Rev. D **106**, 063506 (2022), 2203.16285.

[25] M. Kerscher and J. Weller, arXiv e-prints arXiv:2408.02063 (2024), 2408.02063.

[26] M. Raveri, C. Doux, and S. Pandey, arXiv e-prints arXiv:2409.09101 (2024), 2409.09101.